JOURNAL OF THERMOPHYSICS AND HEAT TRANSFER
Vol. 14, No. 2, April–June 2000

Temperature Measurements by Laser-Induced Fluorescence Spectroscopy in Nonequilibrium High-Enthalpy Flow

Antonio Del Vecchio* and Giuseppe Palumbo†
Centro Italiano Ricerche Aerospaziale, 81043 Capua (CE), Italy
and
Uwe Koch‡ and Ali Gülhan‡
DLR, German Aerospace Research Center, D-51147 Cologne, Germany

The flowfield generated by the high-enthalpy arcjet facility L2K, simulating the stagnation conditions during shuttle reentry and mainly used for testing thermal protection materials, is investigated by using the laser-induced fluorescence (LIF) diagnostic technique. For the operation conditions of the L2K facility of DLR, the flow conditions are dominated by nonequilibrium effects. In particular, translational and rotational temperatures are assumed to be in equilibrium, but large differences between rotational, vibrational, and electronic temperature occur. Spatially resolved LIF is used to determine rotational and translational temperature of NO molecules and O atoms in the freestream and behind a bow shock upstream of a blunt body. The flow is modeled numerically using a quasi-one-dimensional code and a full Navier–Stokes two-dimensional axisymmetric code. Good agreement is achieved between the experimental and numerical data in the freestream. The data are also compared with the coherent Stokes anti-Raman scattering measurements performed previously at the same flow conditions in the same facility on the N_2 molecules. Differences caused by the nonequilibrium aspects, in the freestream and across the shock layer, of N_2, NO, and O components are evident, and the physical interpretation is discussed.

Nomenclature

A_{ki} = spontaneous radiative decay or Einstein coefficient
E_{rot} = rotational energy
E_{trans} = translational energy
E_{vib} = vibrational energy
H_0 = stagnation enthalpy
I_{ki} = intensity of fluorescence
J = total quantum number
k = excited state
k_{BOLTZ} = Boltzmann constant, $k = 1.3806 \times 10^{-23}$ J/K
k_{i-k} = quenching rate
N_k = number density of the excited state k
N_0 = total number density
n_i = number density of the quencher i
P_{rt} = Prandtl number
P_0 = stagnation pressure
Q_k = quenching rate
q_k = fluorescence quantum yield
R = radius of the cylindrical blunt test model
r = internuclear distance
T = temperature
T_{rot} = rotational temperature
T_{vib} = vibrational temperature
Δ = standoff distance
ε = freestream/shock-layer density ratio
ν_{ki} = frequency of the exciting photon
ψ_k = wavefunction of the state k

Received 6 May 1999; presented as Paper 99-3598 at the AIAA 30th Fluid Dynamics Conference, Norfolk, VA, 28 June–1 July 1999; revision received 29 October 1999; accepted for publication 29 October 1999.

*Research Scientist, Hypersonic Department, Via Maiorise. Member AIAA.
†Research Scientist, Hypersonic Department, Via Maiorise.
‡Research Scientist, Plasmawindtunnel Department, Linder Höhe. Member AIAA.

Introduction

THE simulation of spacecraft reentry conditions in a high-enthalpy facility represents one of the most interesting fields of application in both the Centro Italiano Ricerche Aerospaziale (CIRA) and DLR aerospace research programs. In fact, physical and chemical processes, which take place during the reentry phase of aerospace flight, are extremely important for the design of thermal protection materials of reusable spacecraft. The qualification of thermal protection materials under reentry conditions is frequently performed in arc-heated facilities, and, for this purpose, the development of efficient and applicable methodologies of investigation is mandatory.

A main goal is the measurement of the concentrations and physical properties of chemical species in nonequilibrium high-enthalpy flow produced by the arc-heated facility L2K of DLR or the future Scirocco-PWT facility of CIRA. For these reasons, the use of nonintrusive diagnostic techniques for the characterization of the hypersonic and arcjet flows is strongly required to perform a detailed description of the thermodynamic state and a theoretical study of the physical properties of high-enthalpy flows, dominated by nonequilibrium phenomena. Computational fluid dynamics (CFD) and experimental techniques are used to improve the understanding of these complex phenomena. For this purpose, conventional and nonconventional spectroscopic advanced techniques of spontaneous or induced radiation are very promising. Among these, laser-induced fluorescence (LIF) is one of the most powerful methods to measure temperature, pressure, velocity, and concentration of the chemical species in flows.

The main advantages of the LIF technique are its high sensitivity and the selective analysis of the chemical gas composition. However, the large number of parameters, such as laser source, detector system, optical setup, and theoretical data reduction, requires a full and precise optimization.[1–5] For this reason, in order to optimize the LIF diagnostic technique, the availability of a suitable facility with a long operation time, easy access to probe volume and relative low operation cost, such as the L2K wind tunnel at DLR-Cologne, represents an important chance to exploit.

In the present paper, the flowfield properties of high-enthalpy flows have been measured using spatially resolved LIF spectroscopy. The experimental investigations reported in this work are performed

at the nozzle exit and at the position where the test model is placed during the shock-layer measurements. The LIF technique allows the measurement of rotational and translational temperatures of NO molecules and O atoms with excellent spatial resolution. Of particular interest is to map, by using the fluorescent emission of the NO molecule and O atoms, the rotational temperature variation inside the shock layer, which forms in front of the model caused by the shock generated by the interaction of the freejet with a blunt body.

Theoretical Background

The knowledge of physical and chemical properties of plasma flow produced by an arcjet is of fundamental importance to understand better the theoretical basis of the phenomena occurring in a high-enthalpy gas in a nonequilibrium thermodynamic state. For these purposes, in order to study, in a selective way, the chemical-physical state of the gas components, the utilization of the LIF technique requires the analysis and the definition of the atomic/molecular transitions that one intends to investigate.

The detection of oxygen atoms is performed via LIF from the ground electronic state $2p^3P_{2,1,0}$ to the excited level $3p^3P_{2,1,0}$ using a two-photon process (see Fig. 1) and detecting the fluorescence radiation at approximately 845 nm caused by the deexcitation $3p^3P_{2,1,0} \rightarrow 3s^3S_0^1$.

Because of the nonlinear feature of the considered excitation process of the two-photon transition for the oxygen atoms, one must take care about the existence of other optical phenomena that should compete with the process under analysis and change (partially) the electronic population of the excited levels during the LIF.

In the case of the application of LIF to the NO molecule, the technique is based on the excitation of a molecule with laser light, which matches the possible energy differences of their energy levels. After excitation the molecule returns to its ground state by emitting red shifted radiation or by thermal relaxation caused by collisions with other molecules. Under conditions where all of the excited molecules return to the lower states by radiation, the emitted intensity is directly proportional to the density of the molecules within the lower energetic state. For an excitation spectrum, the intensity of the emitted light is recorded as a function of the wavelength of the excitation light, thus probing different densities of the lower energetic states of the molecules. Figure 1 shows the physics of the LIF process for recording excitation spectra.

The modeling of the radiation spectra is performed by assuming a stationary population density in each excited state[6] and the corresponding intensity of the spectral line of the transition from state $\boldsymbol{k}$ to state $\boldsymbol{i}$ proportional to this number density N_k:

$$I_{\mathrm{ki}} \propto N_k h \nu_{\mathrm{ki}} A_{\mathrm{ki}} \tag{1}$$

The A_{ki} Einstein coefficient is proportional to the matrix element $|\langle \psi_k \cdot \boldsymbol{r} \cdot \psi_i \rangle|^2$ and, considering the Born–Oppenheimer approximation and the separation of the wave function into three separate terms (i.e., electronic, vibrational, and rotational factors, $\psi = \psi_{\mathrm{el}} \cdot \psi_{\mathrm{vib}} \cdot \psi_{\mathrm{rot}}$), the A_{ki} coefficient results to be proportional to the coupling of the electronic states M_{ik}, the Franck–Condon factor $q_{v^i v^k}$, and the Hönl–London factor $S_{J^i J^k}$:

$$A_{\mathrm{ki}} \propto M_{\mathrm{ki}} S_{J^i J^k} q_{v^i v^k} \tag{2}$$

To consider different rotational and vibrational temperatures of the molecules, we assume the dependence of the number density N_k of the excited level proportional to two correspondent terms as follows:

$$\frac{N_k}{N_0} \propto \frac{1}{Q_{\mathrm{vib}}} \exp\left(-\frac{E_k^{\mathrm{vib}}}{k_{\mathrm{BOLTZ}} T_{\mathrm{vib}}}\right) \frac{1}{Q_{\mathrm{rot}}} \exp\left(-\frac{E_k^{\mathrm{rot}}}{k_{\mathrm{BOLTZ}} T_{\mathrm{rot}}}\right) \tag{3}$$

By considering relations (2) and (3) into relation (1), we obtain

$$I_{\mathrm{ki}} \propto \frac{1}{Q_{\mathrm{vib}} Q_{\mathrm{rot}}} \exp\left(-\frac{E_k^{\mathrm{vib}}}{k_{\mathrm{BOLTZ}} T_{\mathrm{vib}}}\right) \exp\left(-\frac{E_k^{\mathrm{rot}}}{k_{\mathrm{BOLTZ}} T_{\mathrm{rot}}}\right) S_{J^i J^k} q_{v^i v^k} \tag{4}$$

The terms Q denotes the partition function and S_{JJ} and q the Hönl–London and Franck–Condon factors. Different rotational and vibrational temperatures of the molecules can be considered by separating the corresponding terms in relation (4).

For the operation conditions of the L2K facility, the flow conditions are dominated by nonequilibrium effects.[7] In particular, translational and rotational temperatures are assumed to be in equilibrium, but large differences between rotational, vibrational, and electronic temperatures are expected.

The parameters in Eq. (4) are taken from the literature.[8–11] The molecular band system investigated in the wavelength range of interest (220–240 nm) corresponds to the γ-(0,0) and γ-(0,1) band related to the transition from the fundamental level $X\ ^2\Pi$ to the $A\ ^2\Sigma$ level (see Fig. 1). The Hönl–London factors S_{JJ} are calculated according to the formulas given by Bennett.[12]

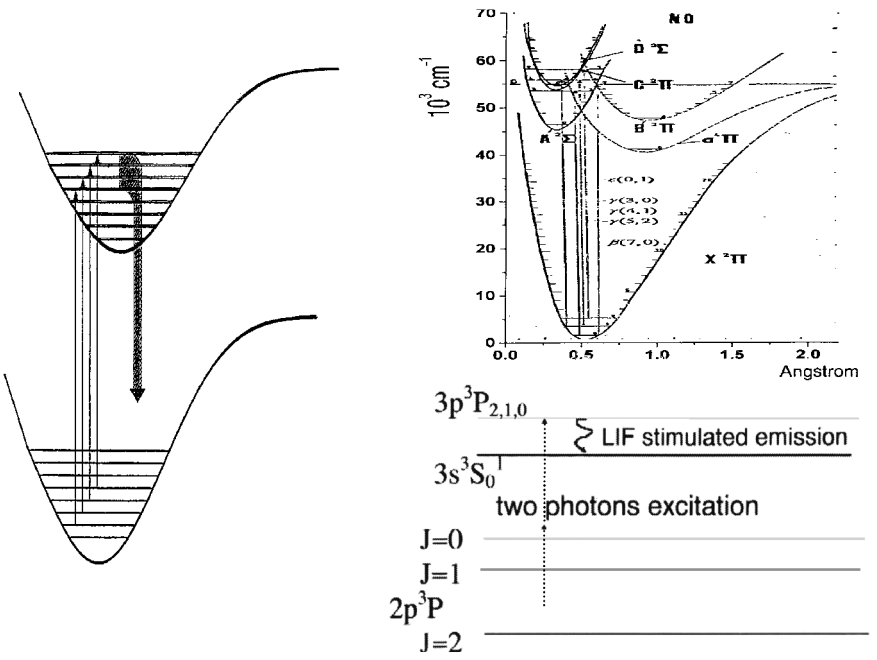

Fig. 1 Schematic diagram of the physical mechanism and energy level diagram of the nitric oxide NO and oxygen atoms O involved in the LIF.

The advantages of using the dye laser system compared to excimer laser are the large number of single lines and spectral separation of transitions from different vibrational ground states. The upper energy levels reached by pumping the fundamental and first excited vibrational level are the same. No influence of the spectral response of the detection system will be present.

At high densities the linearity between the LIF signal and the number density in a special rotational state has to be proven. The loss of linearity may be caused by different effects, such as predissociation or internal conversion, but, at the pressure values of interest, the most critical source for linearity loss should be identified in the collisional quenching.[13,14] This phenomenon is described by the quenching rate Q_k indicating the decreasing of the excited state density N_k caused by collisional processes:

$$\frac{dN_k}{dt} = -Q_k N_k \tag{5}$$

with

$$Q_k = \sum_i k_{i-k} n_i \tag{6}$$

The term n_i is the number density of the quencher elements i, the sum is over all quencher elements, and k_{i-k} is defined as the quenching rate constants depending on the impacting molecule (quencher) i and on the fluorescing state k of the quenched molecule.

Taking into account this contribution of the nonradiative (quenching) decay Q_k to the total decay $Q_k + A_k$ of the excited state k, the fluorescence intensity is reduced by a factor

$$q_k = A_k/(A_k + Q_k) \tag{7}$$

called *fluorescence quantum yield*, and it represents the reduction ratio of the fluorescence intensity caused by the quenching effects.

To evaluate the effect of the quenching reduction on the fluorescence intensity, by assuming the calculated concentrations of the molecules and atoms in the flowfield, the quantum yield q_k can be evaluated. The details of the calculation are reported elsewhere.[15] Briefly, we consider the properties of the freestream flow in the two measurement positions of interest: 1) close the nozzle exit corresponding to the distance of 470 mm from the nozzle throat; and 2) at the center of the test chamber where the test model is positioned during the shock-layer investigations corresponding to the distance of 955 mm from the nozzle throat.

The quenching constants for O atoms, by using the estimated number densities, is 7.1×10^5 s^{-1} for the 955-mm case and 2.5×10^6 s^{-1} for the 470-mm case. Using the decay constants given by Ref. 16 of 2.5×10^7 s^{-1}, the quantum yield for oxygen-atoms is 98% for the 955-mm case and 92% for the 470-mm case.

The quenching constant for the NO molecules, by summing the contribution of all quenchers, is 2.5×10^5 s^{-1} for the 955-mm case and 6.2×10^5 s^{-1} for the 470-mm case. With a decay constant of 4.6×10^6 s^{-1} for the A state, the quantum yield for nitric oxide molecules results to be 96% for the 555-mm case to 92% for the 70-mm case.

Following these considerations, the quenching effect on the radiation intensity in the freestream conditions may be considered not predominant.

For what concerns the evaluation of the quenching in the shock-layer region and by using the same decay constants and the calculated number densities, we obtain an estimated quantum yield for O atoms and NO molecules of 50 and 61%, respectively.

The synthetic spectra are calculated according to the procedure described in Ref. 17. The transition frequencies for the tuning range of the laser were taken from Refs. 10 and 11. The uncertainty of these transitions is claimed to be better than 0.0015 nm, and good agreement with measured transitions could be found. The procedure allows different values for rotational and vibrational temperature to be prescribed. Furthermore, to make comparison with an experiment, the linewidth parameter, related to the spectral linewidth of the exciting laser (in our case 0.0015 nm), could be adapted, and intensities for the full spectra could be calculated.

In Fig. 2 the theoretical curves of the fluorescence emission, in the wavelength range of interest (222.5–237.5 nm) for three different temperatures ($T_{rot} = T_{vib}$ = 450 K, 1500 K, 3500 K), are shown. The appearance of the first excited vibrational band γ-(0,1) begins to be evident in a valuable way for temperatures above 450 K. In particular, the temperature value of 500 K is assumed as the lower limit of the sensitivity of our LIF system in the actual configuration for what concerns the measurement of the vibrational temperature through the detection of the NO γ-(0,1) vibrational band; this limit is evaluated by LIF measurements performed on an heated static test cell filled with a low pressure mixture of N_2 and NO gases and considering the detection of a value greater than 5% of the integrated intensity ratio between the γ-(0,1) and γ-(0,0) NO molecular bands as the limit to obtain an error on the vibrational temperature estimation lower than 10%.

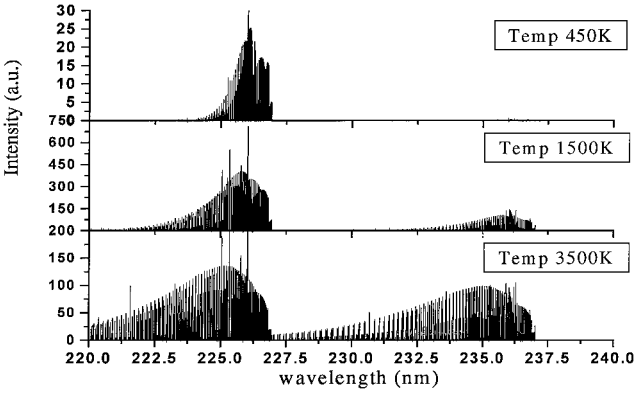

Fig. 2 Theoretical excitation spectra calculated for temperatures of 500, 1500, and 3500 K.

Numerical Simulation

The numerical simulations are performed by using two different codes: NATA and H2NS.

The NATA program is based on a quasi-one-dimensional flow through a nozzle of specified geometry, as described in detail in Ref. 7. The theoretical gas model is based on the mixture of atoms, atomic ions, diatomic molecules, molecular ions, and electrons. In the argon-free air model for low and moderate temperatures, NO^+ is the only important ion among the other species N_2, O_2, N, O, NO, and electrons e. At higher temperatures above 6000 K, four additional ions like N_2^+, O_2^+, N^+, and O^+ are additional species. N_2, N, N^+, N_2^+, and e are the components of the nitrogen model. Reaction-rate coefficient and equilibrium constants are expressed as functions of temperature. Rate coefficients of backward reactions are defined as the ratio of the forward-rate coefficients and the equilibrium constants. The calculations of the thermal species properties assume that the vibrational degrees of freedom of molecules are in thermal equilibrium with the other degrees of freedom.

Regarding the reservoir condition, the flow is always assumed to start from a state of thermochemical equilibrium in an upstream reservoir. The mass-flow rate and stagnation pressure are directly measured quantities in the L2K experiments, and, hence, they are used as the input parameters.

The numerical code provides inviscid frozen, equilibrium, and nonequilibrium flow solutions. The nonequilibrium solution is obtained under the basic approximation of a quasi-one-dimensionality of the flowfield. The species concentrations are governed by chemical rate equations. The solution is started by treating the nonequilibrium flow as a perturbed equilibrium flow. The perturbation method is used until the departure from equilibrium has become large enough to allow the use of numerical integration of the rate equations together with the differential equations of conservation of mass, momentum, and energy.

Regarding the boundary-layer characterization, for most operating conditions of the L2K, the layer is expected to be laminar. The code contains an approximate laminar boundary calculation based on the integral method developed by Cohen and Reshotko (Ref. 7 and all references therein).

Table 1 Calculated test conditions in L2K, NATA code

Quantities for input				
Mass-flow rate, g/s	30		49	
Stagnation pressure, kPa	85		129	
Distance between model and nozzle throat, mm	470	955	470	955
Diameter of the nozzle throat, mm	29			
Diameter of the nozzle exit, mm	200			
Calculated quantities				
Stagnation enthalpy, MJ/kg	8.85		7.16	
Stagnation temperature, K	4386		3874	
Frozen temperature in the freestream, K	430	259	403	243
Equilibrium temperature in the freestream, K	598	357	569	340
Total density in the freestream, 10^{-4}kg/m^3	2.79	0.90	4.68	1.44
Enthalpy, MJ/kg			2.91	2.67
Static pressure, Pa	57.1	11.0	86.4	15.9
Frozen Mach number	5.79	7.67	5.69	7.54
Velocity, km/s	3.14	3.23	2.91	3.00

The main results calculated on the flow centerline are presented in Table 1.

The H2NS code is a flow simulator completely developed in CIRA. It has had a long-time validation since 1993 by various comparison with experimental. The H2NS code has been mainly developed to calculate flowfield and thermodynamic properties at hypersonic regimes. It solves the fully Navier–Stokes equations for two-dimensional and axial-symmetric flows, which can be used to simulate the gas behavior into the nozzle and around the test model of our interest. The spatial discretization of the Navier–Stokes equation system has been made by means of a finite volume technique with a central formulation over structured mesh. The H2NS code consider the air mixture gas composed by the main five species: O, N, NO, O_2, and N_2. It simulates the gas in chemical and vibrational nonequilibrium conditions. Five different chemical models have been implemented: Park in 1985,[18] Park in 1989,[19] Evans Huber–Schexnayder,[20] Kang-Dunn,[21] and Park–Rakich.[22] The vibrational nonequilibrium model is the one proposed by Millikan and White.[23] To take into account the turbulence of the flow, an algebraic two-layer model has been employed. In particular, the turbulent viscosity is derived using the Baldwin–Lomax turbulence model,[24] and the turbulent heat-conduction coefficients are computed using the Prandtl number definition ($Pr_t = 0.9$).

The details of the vibrational model considered for the simulation are reported in Ref. 25, whereas for the chemical model we refer to the one described in Ref. 26.

The two test conditions considered for the calculation are as follows:

1) $P_0 = 0.850$ bar $H_0 = 8.85$ MJ/kg TEST CASE 30 g/s; wall temperature = 300 K (not catalytic).

2) $P_0 = 1.290$ bar $H_0 = 7.30$ MJ/kg TEST CASE 49 g/s; wall temperature = 300 K (not catalytic).

The main results calculated on the flow centerline are presented in Table 2.

Table 2 Calculated test conditions in L2K, H2NS code

Quantities for input				
Mass-flow rate, g/s	30		49	
Stagnation pressure, kPa	85		129	
Distance between model and nozzle exit, mm	70	555	70	555
Stagnation enthalpy, MJ/kg	8.85		7.30	
Calculated quantities				
Stagnation temperature, K	4362		3870	
Rotational-translational temperature in the freestream, K	483	277	467	268
Vibrational temperature of NO in the freestream, K	1082	1070	924	910
Total density in the freestream, 10^{-4} kg/m^3	3.25	0.95	5.46	1.54
Enthalpy, MJ/kg	4.28	4.05	3.31	3.10
Static pressure, Pa	53.6	9.0	83.3	13.4
Frozen Mach number	6.17	8.35	6.03	8.17
Velocity, km/s	3.03	3.10	2.83	2.90

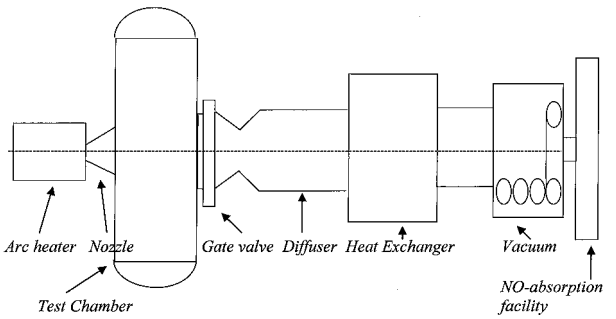

Fig. 3 Schematic layout of the L2K arc-heated facility.

Test Facility and Optical Setup

The LIF experiments described in this paper are performed in the flowfield of the high-enthalpy L2K facility at DLR Research Center in Cologne, Germany. The L2K arc-heated facility is mainly used to test thermal protection materials,[17] offering a wide choice of flow conditions to simulate the stagnation conditions during shuttle reentry. A schematic layout of the arc-heated plasma wind tunnel is shown in Fig. 3.

The facility consists of a gas supply system and a heating system, where the test gas is heated to the desired energy levels and a nozzle (40 cm in length, 2.9 cm in throat diameter, and 20 cm in nozzle exit diameter) to expand the gas to hypersonic Mach numbers. This high-speed flow enters the test section where the cylindrical blunt test model (radius $R = 25$ mm) is mounted. Downstream of the test section the flow is decelerated in a diffuser and cooled in a heat exchanger. As the pressure level is below atmospheric, the gas has to be pumped back to ambient in a vacuum system that can consist of four mechanical pumps. The vacuum system can be separated by a gate valve from the upstream part in order to be able to keep the vacuum while working in the test chamber. Downstream of this vacuum system the installation has a device to wash out pollutants before releasing the gas into the atmosphere.

The arc heater is a Huels type with two hollow electrodes placed on the flow axis heating the test gas injected tangentially to the electrodes with a mass-flow rate between 5 and 75 g/s. Moderate specific enthalpies up to 10 MJ/kg are achieved at a gas mass-flow rate of 50 g/s, i.e., a reservoir pressure of about 1.5 bar. The high-enthalpy hypersonic gas behind the test chambers is decelerated by a diffuser with a central body to recover the pressure before the entrance in the heat exchanger.

The mass-flow rates considered for the measurements reported in this work are 50 and 30 g/s with a power level of about 0.7 MW and a reservoir pressure of 1.29 and 0.85 bar, respectively.

The main components of the optical setup are a tunable excimer laser (Lambda Physics LPX150) pumping the dye laser system (Scanmate 2E, Lambda Physics) and the detection system. The excimer laser is operated with ArF in the broadband mode to emit light pulses with a wavelength of 351 nm and duration of 23 ns, with energy of 200 mJ per pulse. The light from the excimer laser is used to pump the dye laser. The dye used is Coumarin 470, which emits blue light in the range from 440 up to 460 nm. Finally, light pulses with an energy of 5–7 mJ per pulse and a linewidth of 0.0015 nm could be generated in the range of 220–240 nm by using a frequency doubler (BBO- Beta barium borate) and separating the UV radiation from

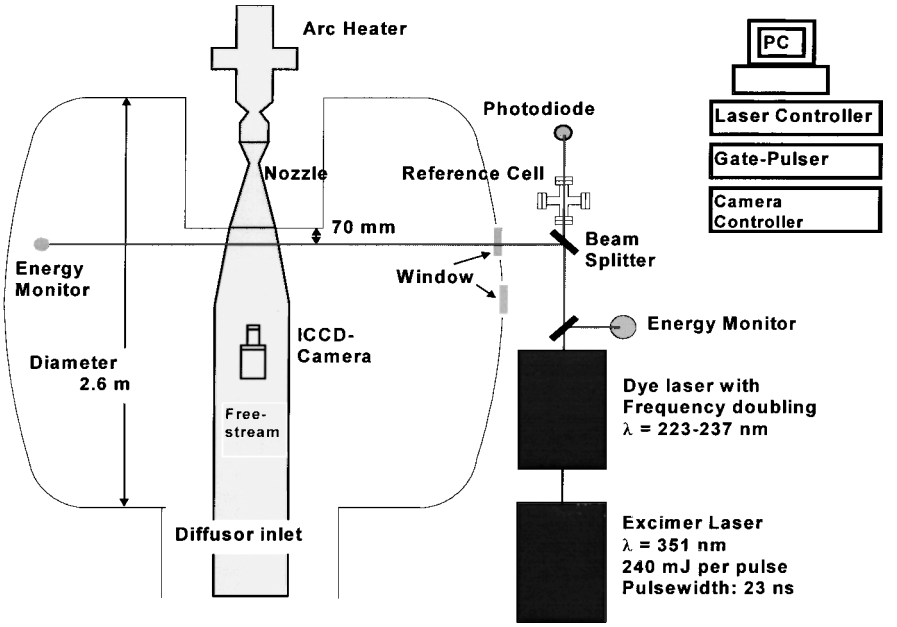

Fig. 4 Typical optical setup used for the spatially resolved LIF measurements.

the residual blue light. The dimension of the focused beam laser results to be less than 1 mm of diameter.

A sketch of one typical optical setup at L2K is reported as in Fig. 4. All of the details of experimental layout configurations, instruments, calibration tests, etc., are reported in Ref. 27.

The light path between the laser and the test chamber is directed on the flow axis in front of the model by using a prism or a beam splitter. No focusing optics are used for freestream measurements to avoid saturation effects in the case of NO measurements, whereas, in the case of O atoms detection, a quartz lens with 1.5-m focus is used to focus the beam to the measurement volume. In front of the test chamber window, a beam splitter is installed. The reflected light is used to monitor the power of each laser pulse with a photodiode, which is referenced to a calibrated power meter (Lambda Physik).

The fluorescence is imaged with $f/4.5$ UV Nikkor lenses onto a cooled intensified charge-coupled device (CCD) camera (Princeton Instruments) with a 384 by 578 pixel array mounted perpendicular to the laser sheet. For NO detection an UG5 filter (Schott) placed in front of the lens blocks the scattered laser light as well as the visible emission from the test gas and the model. For O-atom detection an interference filter with a maximum transmission at 850 nm is used.

Experiments are performed by scanning the full tuning range of the laser with wavelength increments of 0.0005 nm at a repetition rate of 3 Hz. Synchronization of the laser pulse and camera illumination is performed with a photodiode and controlled with an oscilloscope. The illumination time (gate) of the CCD camera is set to 350 ns to collect almost all fluorescence radiation from the considered NO excited level characterized by a lifetime of 217 ns (Ref. 28). To avoid detection of parasitic emission from the model, the laser pulses are synchronized to the illumination interval. As just reported, experimental investigations are performed at a location of 955 and 470 mm downstream of the nozzle throat.

The fluctuation of the intensity variation was checked for the full tuning range of the dye laser setup. Less than 8% shot-to-shot variation of the laser intensity was measured. The laser power was varied by a factor of 10 to prove the linearity of the signal with laser power.

Experimental Results and Discussion

An automatic data reduction procedure was used to extract the temperature information from the measured spectra. In particular, the experimental spectra are corrected by the background signal and the laser power fluctuations; then, the identification of the peaks (the parameters for the identification process, such as the maximum distance between experimental and theoretical position or the signal-to-noise ratio, are settable) are performed comparing the position and the relative intensity ratio of each peak with the theoretical values, and the integrated intensity of identified peaks are calculated. Finally, the data are reduced to Boltzmann plots to obtain the temperature measurement.

The relative uncertainty on temperature measurement $\Delta T/T$ is mainly caused by the error $\Delta I/I$ on the calculation of the integrated intensity of each identified transition peak, properly propagated through the Boltzmann plot fitting procedure, and it may be reduced by extending the analysis to the levels with higher energy differences ΔE through the relation $\Delta T/T \propto T/\Delta E \cdot \Delta I/I$ (Ref. 27).

O-Atoms Measurements

The detection of oxygen atoms is performed via LIF from the ground electronic state $2p^3P_{2,1,0}$ to the excited level $3p^3P_{2,1,0}$ using a two-photon process and detecting the fluorescence radiation at approximately 845 nm because of the deexcitation $3p^3P_{2,1,0} \rightarrow 3s^3S_0^1$ (Ref. 29). The radiation is collected perpendicularly with respect to flow centerline and laser path by a CCD camera equipped with a filter at 850 ± 10 nm (transmittance ≈ 75%).

The considered excitation process of the two-photon transition for the oxygen atoms is a nonlinear effect, and in these cases when no other competitive process that may change (partially) the electronic population of the excited levels is involved, a quadratic dependence of the LIF signal is expected varying the energy of laser pulses. To determine this low-intensity regime, we varied the laser pulse energy in the range about 1.0–3.0 mJ and detected the LIF signal caused by the O-atom transition $2p^3P_{2,1,0} \rightarrow 3p^3P_{2,1,0}$ at 225.60 nm (Fig. 5). The quadratic dependence is observed nearly in the full range except at the very high-energy pulse region where the slope of the dependence decreases. Following these results, it seems reasonable to neglect other competing optical processes.[30]

The LIF measurement are performed in the range 225.5–226.2 nm to detect all of the transitions involved in the $2p^3P_{2,1,0} \rightarrow 3p^3P_{2,1,0}$ for both flow conditions considered in the present test campaign, i.e., (mass-flow rate = 49 g/s ↔ stagnation-pressure= 1290 mbar) and (mass-flow rate = 30 g/s ↔ stagnation-pressure= 850 mbar). In Fig. 6 two typical experimental data sets for the two flow conditions are shown (the intensity of the LIF signals is properly normalized for the laser energy fluctuations). The measurements of O-atom temperature are available only in the freestream 470 mm from the nozzle throat, where the oxygen atom density is the highest one, and, hence, the efficiency of the two-photon process is enhanced.

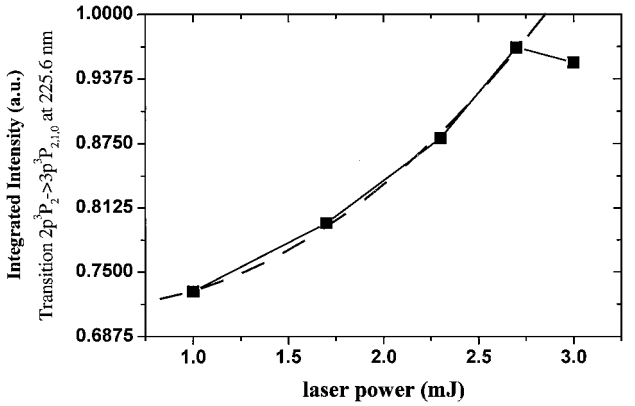

Fig. 5 Integrated intensity of the deexcitation $3p^3P_{2,1,0} \rightarrow 3s^3S_0^1$ caused by the two-photons LIF transition between the levels $2p^3P_2 \rightarrow 3p^3P_{2,1,0}$ vs the variation of the laser power used as excitation source. The second-order least-squares fit (– – –) is performed excluding the last point at 3.0 mJ.

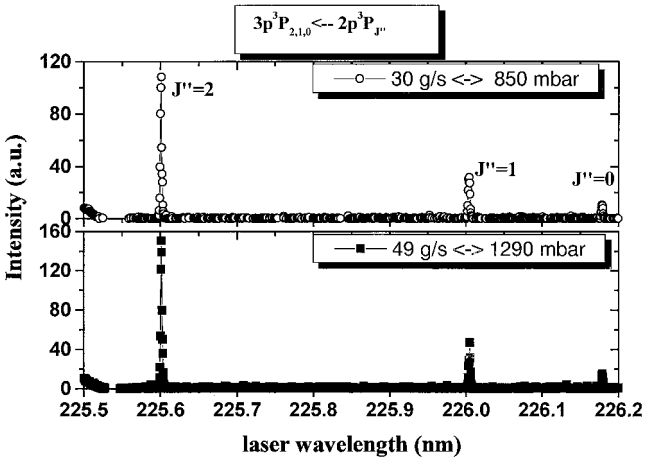

Fig. 6 Collected spectra of the fine structure of the oxygen levels caused by the two-photon excitation $2p^3P_{J''} \rightarrow 3p^3P_{2,1,0}$ for the two flow conditions under analysis: (49 g/s ↔ 1290 mbar) and (30 g/s ↔ 850 mbar).

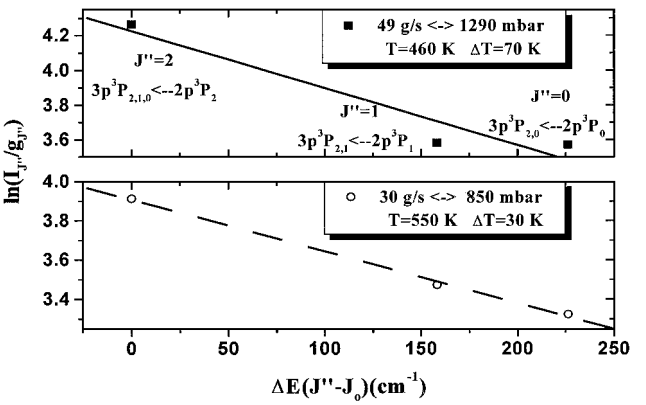

Fig. 7 Typical Boltzmann plots for the two different flow conditions. In the case of (49 g/s ↔ 1290 mbar) (upper graph), the best linear fit is obtained with a temperature of 460 K ± ΔT = 70 K. In the other case (30 g/s ↔ 850 mbar) (lower graph) a temperature of 550 K ± ΔT = 30 K is calculated.

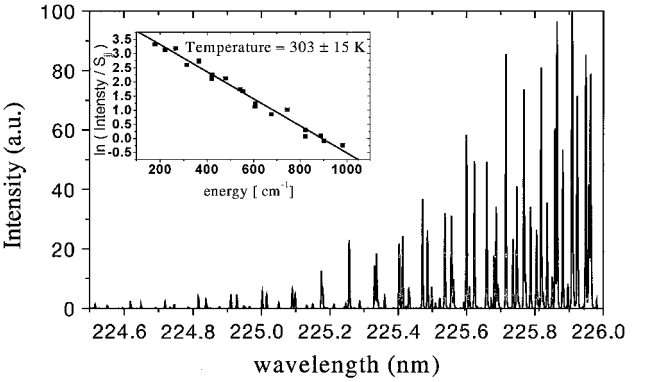

Fig. 8 Freestream spectrum from the flowfield in L2K: mass-flow rate 50 g/s, stagnation pressure 1290 mbar, distance to the throat 955 mm. In the inset the Boltzmann plot and the best linear fit are reported. The temperature calculated results are 303 K ± 15 K.

The fine structure of the $2p^3P_{J''}$ states is evident, and the decreasing intensity as J'' decreases is a confirmation of the lower population of the higher energy levels.

To obtain the estimation of the temperature from the O-atoms LIF signal, we plot the natural logarithm of the integrated intensity normalized by the multiplicity vs the energy difference of the transition levels: the slope of the best fit to straight line in these Boltzmann plots is directly correlated with the temperature. In Fig. 7 two typical Boltzmann plots referred to the two considered flow conditions are reported. For all of the cases corresponding to the condition (mass-flow rate = 49 g/s ↔ stagnation-pressure= 1290 mbar) we obtain a temperature value of about 460 K with an error of 15% (≈70 K). In this case the relative high amount of the error is caused by the intensity of the transition from the $2p^3P_0$ level that is constantly higher than the expected one, but the intensity of this fable peak is affected by a greater relative error than the others; hence, it is needed to measure it with a major degree of accuracy. This represents one of our tasks for future work.

The measured temperature results are in good agreement with the value calculated by the CFD code H2NS. In fact a frozen rotational/translational temperature of 467 K is estimated at 470 mm downstream from the nozzle throat.

In addition to this comparison with the theoretical result, the measured value of the temperature is in very good agreement with the rotational/translational temperature measured using the LIF signal from the NO molecules in the same measurement volume. In fact, as reported in the next paragraph, at 470 mm from the nozzle throat a temperature of 470 K is measured by the NO-LIF analyses, and this consistency, always observed for each flow condition and each measurement position, confirms the character of equilibrium of rotational/translational levels among all chemical species involved in the aerothermodynamic process.

The results for the flow condition corresponding to (mass-flow rate = 30 g/s ↔ stagnation-pressure= 850 mbar) are the following. From the LIF signal of oxygen atoms, a temperature of 550 K is measured, with an error of about 5% (≈ 30 K). The NO-LIF analyses in this flow condition give the measured temperature of 575 K, whereas the H2NS and NATA codes return calculated values of 483 and 598 K, respectively. All of the same considerations of the preceding case are still applicable.

Concluding this section, the application of the LIF technique to oxygen-atom detection in a hypersonic plasma flow is very promising and needs to be optimized. In particular, the measurement procedure and setup should be arranged to increase the sensitivity and, consequently, decrease the relative error. In addition, a dedicated study and analyses have to be performed to reach the objective of quantitative concentration measurement for which the very complex quenching process of O-atoms signal should be taken into account.

NO-Molecules Measurements

Freestream Investigations

The freestream analyses of the LIF signal emitted by the NO molecules have been performed at two different flow-stream locations, i.e., 470 and 955 mm downstream from the nozzle throat.

In Fig. 8 a typical excitation spectra from the freestream at the centerline and the relative Boltzmann plot analysis is reported for

Table 3 Summary of the measured and calculated temperatures

	Mass-flow rate = 30 g/s Measurement position		Mass-flow rate = 50 g/s Measurement position	
Distance from nozzle throat	470 mm	955 mm	470 mm	955 mm
O atom by LIF, K	550 ± 30	n.a.	460 ± 70	n.a.
NO molecule by LIF, K	560 ± 60	320 ± 40	515 ± 30	300 ± 15
N_2 molecule by CARS,[31] K	n.a.	n.a.	n.a.	330
Vibrational frozen/equilibrium by NATA code, K	430/598	259/357	403/569	243/340
Rotational/translational (N_2-O_2-NO) by H2NS code, K	483	277	467	268

the test case (mass-flow rate = 50 g/s ↔ stagnation-pressure = 1290 mbar) at 955 mm downstream from the nozzle throat.

As just discussed, the experimental spectra are analyzed by identifying the NO peaks and by calculating the NO rotational temperature through the Boltzmann plot. The calculated values are about 515 ± 30 and 300 ± 20 K at 470 and 955 mm positions, respectively, in the case (mass-flow rate = 50 g/s ↔ stagnation-pressure = 1290 mbar) and about 560 ± 50 and 320 ± 35 K at 470 and 955 mm positions, respectively, in the case (mass-flow rate = 30 g/s ↔ stagnation-pressure = 850 mbar).

The theoretical results calculated by the computational codes are reported in Table 3, and a good agreement with the data measured with the LIF technique in this work and with the coherent Stokes anti-Raman scattering (CARS) technique in the previous measurements[31] is observed.

In all cases, as no signal from vibrational excited NO molecules is detected, the upper limit of the freestream vibrational temperature NO is estimated below 500 K. The behavior of the vibrational temperature of NO is very different with respect to the case of N_2 as determined by CARS measurements,[31] i.e., Freestream $T_{vib}(N_2) \approx 2700$ K. This effect can be explained with the faster vibrational relaxation of NO with respect to the N_2 molecule and represents an evident consequence of the nonequilibrium thermodynamic state of the gaseous flow.

Shock-Layer Investigations

To perform the analyses on the shock layer, a cylindrical (50 mm diam) test model is inserted in the freestream with the flat (disc) surface in front to the plasma flow, and it is surrounded by a region of high temperature and density caused by the formation of a shock front. The test model position is 955 mm downstream from the nozzle throat.

A gas in nonequilibrium thermodynamic state, as just mentioned, may be described by using three different temperatures of which the most important for the gas-surface interaction is the rotational temperature, because the rotational axis compared to the normal to the surface is an important parameter in determining the thermal load to the surface. Previous CARS measurements[31] had shown a dramatic rise of the rotational temperature of N_2 molecules in the layer up to the body. It is an important finding to reveal and to confirm this result by the LIF method applied to the NO molecule.

A typical radiation spectrum from the shock region is reported in Fig. 9. Because of the high temperature, the profile of the NO-γ(0,0) ($A\,^2\Sigma \leftarrow X\,^2\Pi$) band system is very different with respect to the one obtained during the freestream measurement. In addition, the NO-γ(0,1) band system is visible and emitting, indicating a higher vibrational NO temperature.

The two-dimensional feature of the LIF setup permits us to investigate in the transverse direction with respect to the flow. In Fig. 10 a temperature profile of NO-LIF emission from the transversal line positioned at 4.2 mm from the model surface is reported. The NO rotational temperature is about 4100 K, a value that is even higher than the calculated stagnation temperature (3870 K). Higher rotational temperatures can be explained with the nonequilibrium properties of the flow. With respect to equilibrium conditions, more energy is stored in the rotational modes, whereas the energy stored in the vibrational modes is lower. At the two extremities of the profile,

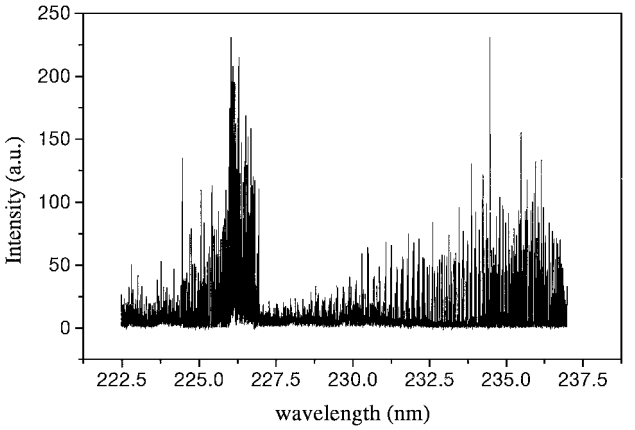

Fig. 9 LIF radiation spectrum in the tuning range of the dye laser (220–240 nm) in the region of the shock in front to the model. The two band systems γ-(0,0) and γ-(0,1) of the transition $A^2\Sigma \leftarrow X^2\Pi$ are visible.

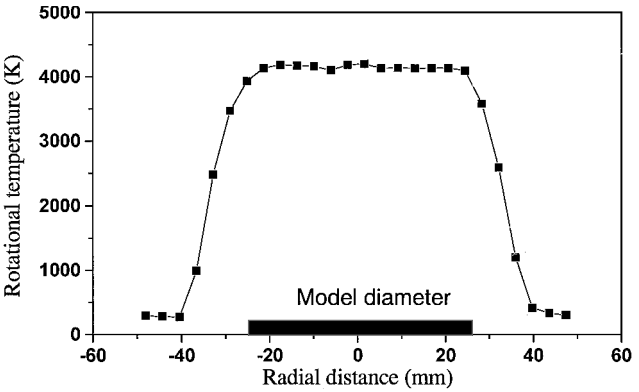

Fig. 10 NO rotational temperature distribution in the transversal direction inside the shock region (4.2 mm from model surface) in the test case (mass-flow rate = 49 g/s ↔ stagnation pressure = 1290 mbar).

the measured rotational temperature corresponds to the unperturbed freestream condition, and the value is exactly matching the measured one in the same position without model inserted.

The measurement of the radiation spectrum from the centerline is repeated for each millimeter of distance from the model surface with a precision of less than 0.5 mm, and the experimental results for the NO rotational temperature on the centerline are reported (Fig. 11). From this graph it is possible to estimate the standoff distance Δ of about 13.5 mm. This experimental value can be compared with the calculated value derived from the formula $\Delta = R\varepsilon^{1/2}(1 + \varepsilon)$ reported in Ref. 32. In the considered flow conditions the density ratio ε is 0.19, and, hence, the calculated standoff distance Δ results are 13 mm, in good agreement with the measured value.

No computational CFD calculation for the plasma flow considering the presence of the model and, hence, of the shock layer in front to the flat surface is available in the test cases considered in this

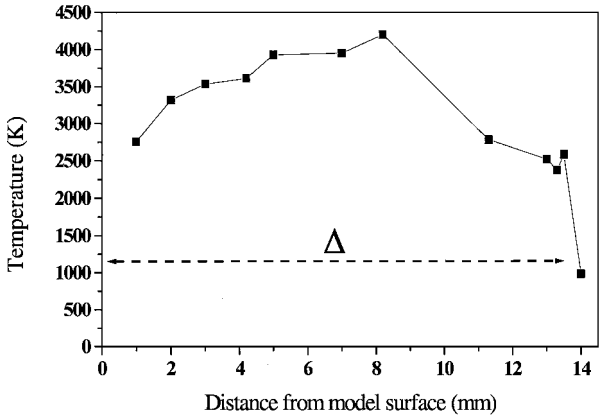

Fig. 11 NO rotational temperature distribution along the centerline inside the shock region generated by the 50-mm-diam test model in the test case (mass-flow rate = 49 g/s ↔ stagnation pressure = 1290 mbar). The standoff distance Δ may be estimated as about 14 mm.

work. In the previous CARS measurement[31] on the N_2 molecule, the measured rotational temperature in the shock region was about 4000 K whereas the vibrational temperature was about 2700 K. The computed values were in good agreement with the experimental ones. As expected, because of the slower vibrational relaxation of the N_2 molecule the vibrational nonequilibrium was demonstrated. Moreover, the vibrational N_2 temperature value remains almost unchanged during the transition from freestream to shock-layer region.

In the case of the NO molecule investigated in this work, the rotational temperature values measured in the freestream and in the shock region are in good agreement with the rotational N_2 temperature indicating an equilibrium of the rotational energy E_{rot} distribution on the different gas components, but, as reported in Table 3, the measured temperature is not consistent with the value expected in the case of a thermal equilibrium indicating thermodynamic nonequilibrium among E_{rot} and other energy forms.

On the contrary, the preliminary results of the vibrational NO temperature values seem to indicate, in this case, an equilibrium in the freestream between rotational and vibrational energy ($E_{rot} = E_{vib}$), whereas the vibrational temperature levels increase in a consistent way across the boundary shock layer [from T_{vib} (NO) < 500 K to T_{vib} (NO) > 2000 K]. The computed values seem to be in good agreement with our results just reported. In the near future a full test campaign and a detailed analysis of the experimental data for vibrational temperature and relative density variation will be performed.

Conclusions

The thermodynamic properties of the plasma flow generated in the L2K arc-heated high-enthalpy facility are investigated by using the spatially resolved LIF technique. In particular, this diagnostic methodology has been applied to the analysis of the NO molecules and O atoms in order to have spatially resolved rotational temperature measurements.

The measured rotational NO temperatures in the freestream are consistent with the O-atom experimental values and N_2 rotational temperatures measured by CARS. In this case the theoretical calculated values are in good agreement with the experimental data. The nonequilibrium aspects are demonstrated by the difference between the measured values and the expected values in the hypothesis of thermal equilibrium.

In the case of the shock-layer investigations in front of a 50-mm-diam test model, spatially resolved measurements of NO rotational temperature are performed. The results indicate temperature values of about 3700 K inside the shock region and a standoff distance of about 14 mm.

In addition, the preliminary results about the vibrational NO temperature indicate a nonequilibrium in the vibrational energy E_{vib} distribution caused by the frozen flow condition combined with the difference in the relaxation process, that is, in the case of the NO molecule, faster than the N_2 air component.

In the future more detailed investigations about vibrational temperatures and relative density variation are foreseen.

References

[1]Beck, W. H., Koch, U., and Müller, M., "Spectroscopic Diagnostic Techniques for the High Enthalpy Shock Tunnel in Göttingen (HEG): Preparatory LIF Studies on Other Facilities," *Proceedings of the NATO Advanced Research Workshop*, edited by A. Boutier, Series E: Applied Sciences, Vol. 224, 1993.

[2]Seitzman, J. M., and Hanson, R. K., "Comparison of Excitation Techniques for Quantitative Fluorescence Imaging of Reacting Flows," *AIAA Journal*, Vol. 31, No. 3, 1993, pp. 513–519.

[3]Hanson, R. K., Chang, A. Y., Seitzman, J. M., Lee, M. P., Paul, P. H., and Battles, B. E., "Laser-Induced Fluorescence Diagnostics for Supersonic Flows," AIAA Paper 90-0625, 1990.

[4]Palmer, J. L., McMillin, B. K., and Hanson, R. K., "Planar Laser-Induced Fluorescence Imaging of Velocity and Temperature in Shock Tunnel Free Jet Flow," AIAA Paper 92-0762, Jan. 1992.

[5]Okabe, H., *Photochemistry of Small Molecules*, Wiley, New York, 1978.

[6]Demtröder, W., *Laser Spectroscopy*, Springer–Verlag, Berlin, 1998, p. 414.

[7]Gülhan, A., and Esser, B., "Numerical Computation of Gas Properties at Characterization Test Conditions," DLR, German Aerospace Research Center, IB-39113-92C32, Cologne, Germany, Dec. 1992.

[8]Huber, K. P., and Herzberg, G., "Molecular Spectra and Molecular Structure," *Constants of Diatomic Molecules*, Vol. 4, Van Nostrand, Princeton, NJ, 1979, pp. 468–483.

[9]Hinz, A., Wells, J., and Maki, A. G., "Heterdyne Frequency Measurement on the Nitric Oxide Fundamental Band," *Journal of Molecular Spectroscopy*, Vol. 119, 1986, pp. 120–125.

[10]Amiot, C., and Verges, J., "Spin Rotation Doubling in the NO Electronic States by Emission Fourier Transform Spectroscopy," *Chemical Physical Letters*, Vol. 66, No. 3, 1979, pp. 570–573.

[11]Amiot, C., and Verges, J., "Fourier Transform Spectroscopy of the $D\ ^2\Sigma^+ - A\ ^2\Sigma^+$ and $E\ ^2\Sigma^+ - A\ ^2\Sigma^+$ Systems of Nitric Oxide," *Physica Scripta*, Vol. 26, 1982, pp. 422–438.

[12]Bennett, R. J. M., "Hönl-London Factors for Doublet Transitions in Diatomic Molecules," *Monthly Notices of the Royal Astronomical Society*, Vol. 147, 1970, pp. 35–46.

[13]Andresen, P., "Laser Induced Fluorescence Imaging Applications," *Measurement Techniques for Hypersonic Flows—Lecture Series 1990-05*, von Kármán Inst. for Fluid Dynamics, Belgium, 1990.

[14]Drake, C. M., and Ratcliffe, J. W., "High Temperature Quenching Cross Sections for Nitric Oxide Laser-Induced Fluorescence Measurements," *Journal of Chemical Physics*, Vol. 98, No. 5, 1993, p. 3850.

[15]Del Vecchio, A., and Palumbo, G., "Quenching Phenomena in Non Equilibrium Hypersonic Flow Generated in an Arcjet Wind Tunnel," Italian Center for Aerospace Research, CIRA-FIP-99-150, Capua (CE), Italy, Sept. 1999.

[16]Bischel, W. K., Perry, B. E., and Crosley, D. R., "Detection of Fluorescence from O and N Atoms Induced by Two-Photon Absorption," *Applied Optics*, Vol. 21, No. 8, 1982, p. 1419.

[17]Gülhan, A., "Arc Heated Facility LBK as a Tool to Study High Temperature Phenomena at Re-Entry Conditions," DLR, German Aerospace Research Center, IB-39113-97A05, Cologne, Germany, Oct. 1997.

[18]Park, C., "On Convergence of Computation of Chemically Reacting Flows," AIAA Paper 85-0247, Jan. 1985.

[19]Park, C., "A Review of Reaction Rates in High Temperature Air," AIAA Paper 89-1740, 1989.

[20]Evans, J. S., Shexnayder, C. J., and Huber, P. W., "Boundary Layer Electron Profiles for Entry of a Blunt Slender Body at High Altitude," NASA TN D-7332, July 1973.

[21]Kang, S. W., Jones, W. L., and Dunn, M. G., "Theoretical and Measured Electron Density Distribution at High Altitude," *AIAA Journal*, Vol. 11, No. 2, 1973, p. 141.

[22]Rakich, J. V., Bailey, H. E., and Park, C., "Computation of Non-Equilibrium Supersonic Three-Dimensional Inviscid Flowfield over Blunt-Nosed Bodies," *AIAA Journal*, Vol. 21, No. 6, 1983, pp. 834–841.

[23]Millikan, R. C., and White, D. R., "Systematic of Vibrational Relaxation," *The Journal of Chemical Physics*, Vol. 39, No. 12, 1963, pp. 3209–3213.

[24]Baldwin, B. S., and Lomax, H. L., "Thin Layer Approximation and Algebraic Model for Separated Turbulent Flow," AIAA Paper 78-257, Jan. 1978.

[25] Park, C., "Review of Chemical Kinetic Problems of Future NASA Missions, I: Earth Entries," *Journal of Thermophysics and Heat Transfer*, Vol. 7, No. 3, 1993, p. 385.

[26] Park, C., and Lee, S. H., "Validation of Multi-Temperature Nozzle Flow Code NOZNT," AIAA Paper 93-2862, July 1993.

[27] Koch, U., Gülhan, A., Esser, B., Grisch, F., and Bouchardy, P., "Rotational and Vibrational Temperature and Density Measurements by Planar Laser Induced NO-Fluorescence Spectroscopy in a Nonequilibrium Shock Layer Flow," Advanced Aerodynamic Measurement Technology, RTO/AGARD, Seattle, WA, Sept. 1997 (Paper 15); also Del Vecchio, A., and Palumbo, G., "Application of the LIF Diagnostic Technique to the Arc Heated Facility LBK (DLR-Cologne)," Italian Center for Aerospace Research, CIRA-TR-97-092, Capua (CE), Italy, July 1997.

[28] McDermid, I. S., and Laudenslager, J. B., *Journal of Quantitative Spectroscopy and Radiative Transfer*, Vol. 27, 1982, p. 483.

[29] Meier, U., Bittner, J., Kohse-Hoinghaus, K., and Just, Th., "Discussion of Two-Photon Laser-Excited Fluorescence as a Method for Quantitative Detection of Oxygen Atoms in Flames," *Twenty-Second International Symposium on Combustion*, Combustion Inst., Pittsburgh, PA, 1988, pp. 1887–1896.

[30] Bamford, J. D., O'Keefe, A., Babikian, D. S., Stewart, D. A., and Strawa, A. W., "Characterization of Arcjet Flows Using Laser-Induced Fluorescence," *Journal of Thermophysics and Heat Transfer*, Vol. 9, No. 1, 1995, pp. 26–33.

[31] Park, C., "Stagnation Point of Flat Disks—Part II: Experiment," *AIAA Journal*, Vol. 21, No. 12, 1983, p. 1748.

[32] Grisch, F., Bouchardy, P., Koch, U., and Gülhan, A., "Rotational and Vibrational Temperature and Density Measurements by Coherent Anti-Stokes Raman Scattering in a Nonequilibrium Shock Layer Flow," Advanced Aerodynamic Measurement Technology, RTO/AGARD, Seattle, WA, Sept. 1997 (Paper 14).